Salt Water Modeling of Fire Compartment Gravity Currents

C. M. FLEISCHMANN
University of Canterbury
Christchurch, New Zealand

P. J. PAGNI and R. B. WILLIAMSON
University of California
Berkeley, CA 94720, USA

ABSTRACT

In order to investigate the gravity current speed and the extent of its mixed region in backdraft experiments, a series of scaled salt water experiments were conducted. The scaling parameters are the Froude number, $v^* = v/\sqrt{\beta g h_1}$, and the normalized density difference, $\beta = (\rho_0 - \rho_1)/\rho_1$, where 1 indicates initial conditions in the compartment (fresh) and 0 indicates conditions in the ambient (salt). The scaled compartment (0.3m x 0.15m x 0.15m) was fitted with a variety of end openings: full, slot, door, and window. Video and photo data indicate that the mixing layer which rides on the gravity current in the full opening case, expands to occupy nearly the entire current in the partial opening cases. Results for the scaled current height, $h^*=h_0/h_1$ and v^* respectively are: full (0.5, 0.44), slot (0.38, 0.32), door (0.33, 0.35), and window(0.29, 0.22). These data are independent of β and are in good agreement with limit calculations from the literature.

KEYWORDS: compartment fires, backdraft, gravity current, salt water modeling, fire initiation, explosion hazards

INTRODUCTION

A gravity current is the flow of one fluid into another caused by a difference in density. This density difference may be due to a dissolved chemical or a difference in the temperature between the two fluids. There are many common examples of gravity currents including sea-breeze fronts, avalanches, lock exchanges, and flows following volcanic eruptions. A large body of research is available on the subject of gravity currents.[1,2] In many cases, the flow field in gravity currents is sufficiently complex that the problem is difficult to solve from first principles. For this reason, physical models, typically salt water models, are used to analyze these problems. Salt water models have been applied to many fire problems including corridor smoke flow, ship board fires, and compartment fires.[3,4]

When a fire occurs in a closed compartment where the only ventilation is due to leakage, the fire initially grows independent of the surroundings and a hot upper layer develops within the compartment. If the leakage rate is small, the hot layer descends over the fire and the burning becomes limited by the available oxygen thus producing large amounts of unburned fuel. Left undisturbed, the heat release rate will decrease and the fire may enter a smoldering stage. When the compartment is opened, a gravity current of dense ambient air enters, mixing with the lighter, fuel rich, compartment gases. If the fuel concentrations are high enough, the mixed region carried with the gravity current may ignite, resulting in a backdraft[5].

This study attempts to quantify the gravity current which enters a compartment prior to a backdraft. A salt water scale model with two different density fluids is used to visualize the flow into the compartment. Because the fire is assumed to be small or smoldering, plume effects are ignored and the compartment is filled with a uniform density fluid lighter than the fluid outside the compartment. Data collected from these experiments include gravity current propagation velocity and geometry. In addition to the entering current, the current which is reflected off the wall opposite to the opening wall is examined.

GRAVITY CURRENT SCALING

As a simplified limit of a gravity current, consider the steady flow of a perfect fluid in a semi-infinite horizontal box of arbitrary width as shown in Fig. 1. At time zero, far to the right, the entire end of the box is instantaneously removed. High density ambient fluid, state 0, flows into the box, as low density compartment fluid, states 1 and 2, flows out, due to buoyancy. The parameter depicting the buoyancy is the normalized density difference,

$$\beta = \frac{(\rho_0 - \rho_1)}{\rho_1}, \tag{1}$$

where ρ_0 is the higher density, ambient, fluid within the gravity current and ρ_1 is the lower density fluid, (at opening) within the hot compartment ahead of the gravity current.

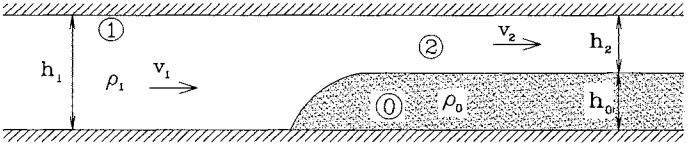

FIGURE 1 - Gravity current schematic. Velocities are indicated in a reference frame fixed on the gravity current. Heights are indicated by h.

Benjamin[1] has shown that, in this perfect fluid limit with no mixing or dissipation, conservation of mass, momentum and energy can be written, respectively, as

$$v_1 h_1 = v_2 h_2, \tag{2}$$

$$v_1^2 h_1 + \beta g h_1^2 = 2 v_2^2 h_2 + \beta g h_2^2, \tag{3}$$

$$v_2^2 = 2\beta g(h_1 - h_2). \tag{4}$$

Eliminating v_1 and v_2, the height of the exiting compartment fluid is

$$h_2 = \frac{h_1}{2} = h_0. \tag{5}$$

This is also the height of the gravity current since $h_0 = h_1 - h_2$. Benjamin[1] shows that for flows with energy losses, $h_0 < h_1/2$. The nondimensional velocity or Froude number of the fluid exiting the compartment is

$$\frac{v_2}{\sqrt{(\beta g h_2)}} = \sqrt{2}, \tag{6}$$

since this is >1 a dissipative hydraulic jump is possible. The velocity of the compartment fluid approaching the gravity current, or in the laboratory reference frame, the gravity current velocity, from Eqs. 2, 5 and 6, is,

$$v^* = \frac{v_1}{\sqrt{\beta g h_1}} = \frac{1}{2}. \tag{7}$$

Thus for scaling, the characteristic dimension and velocity are

$$x_c = h_1 \text{ and } v_c = \sqrt{\beta g h_1}, \tag{8}$$

from Eqs. 5 and 7 respectively. The characteristic time is then

$$t_c = \frac{x_c}{v_c} = \sqrt{\frac{h_1}{\beta g}}. \tag{9}$$

Typical dwellings have room heights of 2.4 m (8 ft). The salt water compartment described here is 0.15 m (0.5 ft) high, so it is 1/16 scale to a dwelling.

The salt water experiments are necessary to quantify the effect of transients, mixing, energy dissipation, opening geometry, and aspect ratio on the simple gravity current size and nondimensional velocity expressions given by Eqs. 5 and 7. They will provide confirmation and corrected formulas useful for modeling backdrafts in fire compartments.

The salt water experiments are limited to $0.003 \le \beta \le 0.101$, while the backdraft compartment and full scale fires produce higher β, up to 1.2. However, the literature suggests,[6] as confirmed by experimental Froude numbers developed here, that v^* is independent of β and depends only on the opening geometry. Therefore, these scaled velocity and geometry results are expected to apply directly to actual and modeled backdrafts. For example, a velocity of 0.09 m/s at a $\beta = 0.05$ for a salt water current in a slot opening geometry gives $v^* = 0.32$,

which would correspond to 0.8 m/s at a $\beta = 0.5$ in the 1.2 m high model compartment and 1.1 m/s at the same β in a 2.4 m high dwelling.

Heat transfer effects at the boundaries and between fluids are not included[3]. Separate analyses and experiments will be required for gravity currents submerged at great depths [1,7] as would occur upon opening a small door in a large, high warehouse.

APPARATUS AND PROCEDURE

Salt water experiments were conducted by placing an acrylic compartment within a larger glass tank. The large tank, 0.3 m wide, 0.6 m long, and 0.45 m deep, contained a dense salt water solution ranging in density from 1.003 kg/m^3 to 1.101 kg/m^3. The solution temperature was 18°C. Densities less than 1.003 kg/m^3 were too difficult to measure accurately and with densities above 1.10 kg/m^3 the solution became opaque making visual observation unreliable.

The compartment was constructed from 6 mm thick acrylic with interior dimensions of 0.15 m wide, 0.30 m long (L) and 0.15 m high. Figure 2a shows the plan and elevation views of the compartment. A flange was built at one end of the compartment so that the opening geometry could be easily modified by replacing a face plate bolted to the flange. Four opening geometries were used. As seen in Fig. 2b, the cross hatched area indicates the opening. The full and slot openings can be considered two-dimensional in the large scale whereas window and door openings are clearly three-dimensional. The end opening was covered with a vertical sliding partition that was removed to start the experiment. The compartment was made negatively buoyant by adding 1.6 kg of lead shot in ballast channels beneath the compartment as indicated in Fig. 2a. The solution in the compartment was regular tap water with: pH 6.8, density 1.000 kg/m^3, and temperature 18°C.

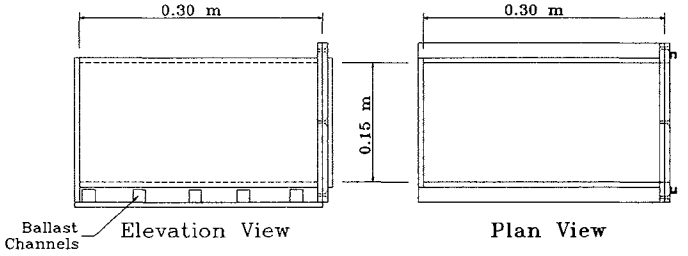

Figure 2a - Sketch of the salt water compartment showing the elevation and plan views.

In the early two dimensional experiments, blue dye was added to the compartment. A small amount of phenolphthalein (4×10^{-5}M concentration) was also added to the compartment fluid to visualize the gravity current mixing. When phenolphthalein mixes with a base, in this case sodium hydroxide, the product of the reaction is red. This reaction is believed to be diffusion limited. The red product is strongly visible even in dilute concentrations. Turbulence is unaffected by the reaction since it produces little surface tension, buoyancy, or heat release. Unlike the passive scalar techniques, such as dye, the chemical reaction of the

phenolphthalein gives a much better indication of the mixing that occurs in the gravity current. A thorough discussion of this technique is given by Breidenthal[8].

In the three dimensional experiments, a mirror was placed above the compartment at a 45° angle to show the plan view of the gravity current in the same plane as the elevation view for video recordings. When the mirror was used, the blue dye was eliminated and the phenolphthalein concentration was increased by a factor of 4 to 1.6×10^{-4}M to produce a more visible gravity current.

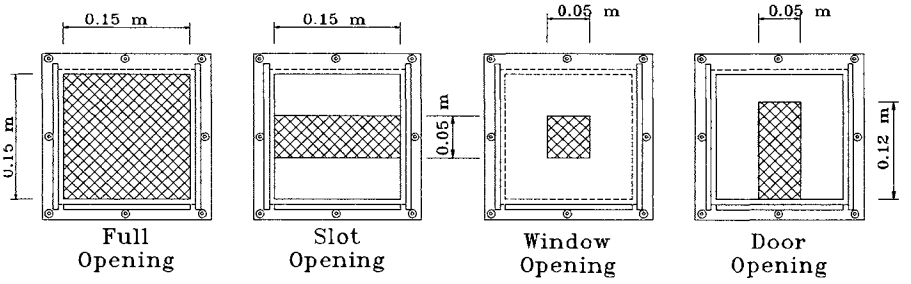

Figure 2b - Sketch of the four opening geometries for the salt water compartment.

Once the two solutions were prepared, specific gravity, temperature, and pH were recorded. The compartment was then lowered into the tank and the partition on the compartment was removed within 120 s to avoid leakage effects. The gravity current was recorded using a high 8 mm video camcorder at 30 frames per second.

COMPARTMENT GRAVITY CURRENT STRUCTURE

Some characteristic features of a steady state gravity current include: a head at the front of the current, mixing at the shear interface between the two fluids, and a series of advancing lobes and clefts at the leading edge. Figure 3 is a simple sketch showing plan and elevation views displaying some of these features on a steady state gravity current. The foremost point of the current is slightly raised above the bottom surface to a height of h_n. This lifting of the head is a result of the faster moving heavier fluid overrunning the slower light fluid. The lighter fluid is forced under the gravity current as a result of the no slip condition at the lower bounding surface.

The overrun fluid causes a gravitational instability which is largely responsible for the three-dimensional effects which are seen in natural gravity currents. The instability is manifested as the lobes and clefts which make up the leading edge of the current and the billows which form above and behind the head of the current[9,10]. In Fig. 3, the plan view of the leading edge shows the lobe and cleft structure. The width of the lobe is $b \sim O(h_0)$ as reported by Simpson[9]. As a lobe widens it will split and a portion of the dense fluid, mixed with the

lighter fluid overrun by the current, is swept up and over the head forming a new billow behind the head of the advancing current. As a result of the split two smaller lobes are formed and a cleft develops between them. The billows which form behind the head of the gravity current are both qualitatively and quantitatively similar to the Kelvin-Helmholtz instability of a shear layer separating two flowing fluids of different densities[6,11].

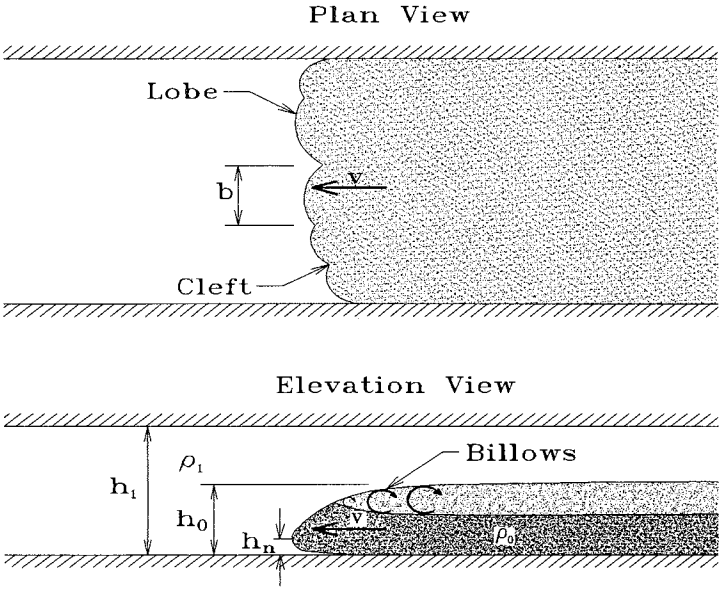

Figure 3 - Sketch of the gravity current with a no slip condition at the lower boundary. Both elevation and plan views are shown. Characteristic features of the gravity current are shown including the lobes, clefts, and billows.

Figure 4a is a photograph showing the gravity current approximately 3L/4 into the compartment for the full open condition. The lower half of the photograph shows the profile of the gravity current. The top half of the photograph shows the plan view reflected in the inclined mirror. The mixed region, confined to a shallow layer between the two fluids along the shear interface, is red due to the chemical reaction of the phenolphthalein but appears gray in the black and white photograph. In profile the gravity current head is raised above the lower boundary as described above. The fluid that is overrun by the current is visible in the photograph as the gray area under the head. Along the interface between the two fluids the large billows can be seen developing behind the head. In plan view the lobes and clefts which make up the leading edge can be clearly seen. The lobes and clefts make the leading edge of the current difficult to determine and contribute significantly to the overall error analysis.

The photograph in Figure 4b of the gravity current approximately 3L/4 into the compartment for the slot opening shows an important conclusion from this salt water modeling. The current is mixed throughout, as indicated by the increased size of the gray (red) region

compared to the full open case. The increased mixing is a result of the rearward facing step caused by the opening being placed above the floor. Otherwise, the profile of the gravity current shows a similar structure to the traditional gravity currents discussed above i.e., the slightly raised head and the billows formed behind the head. The plan view of the current clearly shows the presence of lobes and clefts at the leading edge. The gravity current head is not as high as in the full open case and the lobes are also smaller. The retarding effect of the no slip boundary condition along the walls is also apparent in the plan view.

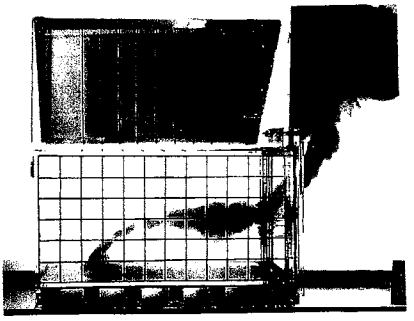

FIGURE 4a - Photograph of the gravity current approximately 3L/4 into the compartment for the fully open condition with $\beta = 0.018$.

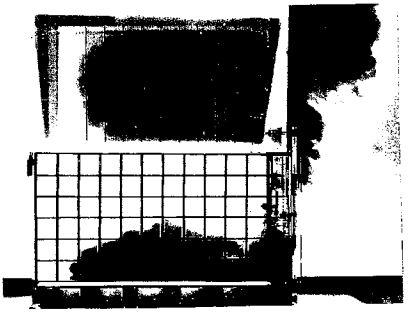

FIGURE 4b - Photograph of the gravity current approximately 3L/4 into the compartment for a center $h_1/3$ horizontal slot opening with $\beta = 0.024$.

Figures 4c & d are photographs showing the gravity currents approximately 3L/4 of the way into the compartment for the window and door opening conditions respectively. By the time the current has reached the 3L/4 point, the effects of the three-dimensional opening are reduced and the gravity current is qualitatively similar to the two-dimensional slot opening. The effect of the three-dimensional opening can be seen in the series of photographs shown in Fig. 5. These photos show how the gravity current enters the compartment for the window geometry. The current initially spreads radially from the opening but by the time the current reaches approximately L/2, the leading edge is moving into the compartment in a similar manner to the slot opening. The three dimensional opening will increase the amount of entrainment that occurs as the fluid cascades over the edges forming the opening. This entrainment is caused by relatively large coherent structures somewhat similar to those occurring in the plume as it exits the compartment.

FIGURE 4c - Photograph of the gravity current approximately 3L/4 into the compartment for a window opening $h_1/3$ square with $\beta = 0.032$.

FIGURE 4d - Photograph of the gravity current approximately 3L/4 into the compartment for a door opening of width $h_1/3$ and height $7h_1/9$ with $\beta = 0.026$.

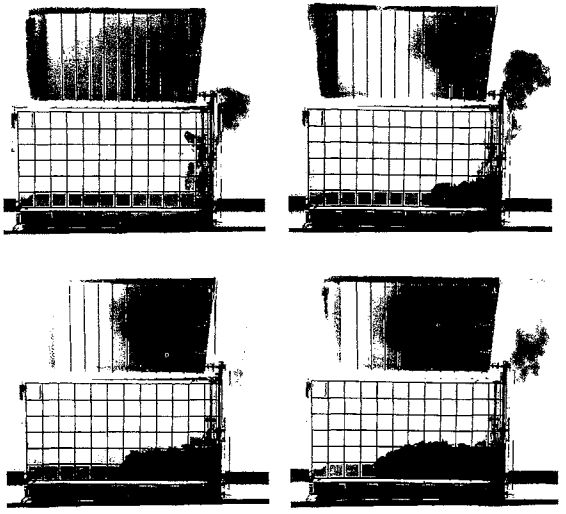

FIGURE 5 - Series of four photographs of the gravity current modeling showing the developing gravity current as it enters the compartment for the window opening β=0.032 at times: 1.4 s, 2.2 s, 3.3 s, 4.6 s.

RESULTS OF SALT WATER MODELING

The experimental nondimensional velocity, Froude Number, Eq. 7, is defined in terms of the gravity current velocity, $v = L/t_{in}$, where t_{in} is the time required for the leading edge of the gravity current to reach the wall opposite the opening. Once the gravity current reaches the rear wall it is reflected up and around until it travels toward the opening. A Froude number is

also calculated for the returning current. The returning gravity current velocity is, $v_e = (2L+2h_1/3)/t_{out}$, where t_{out} is the time from opening to the time the reversed current returns to the opening wall. The $2h_1/3$ factor is used to account for the length the current travels up the rear wall and compares well with video observation of the current stretch up the wall. Using this factor results in v* being nearly equal for both the entering and exiting currents. For the full opening condition it is not possible to determine the leading edge of the returning current because there is no restriction on the exiting flow.

In Table 1, β, t_{in}, v, v*, and Re for the entering wave are given in columns 1 thru 5 respectively. For the exiting current, t_{out}, v_e, and v_e^*, are given in columns 6 thru 8 respectively. Looking at the v* values given in Table 1, it can be seen that the value is constant, differing only with geometry, over the range of β investigated. Figure 6 is a plot of v* versus β for the entering wave for all four opening geometries. The average values of v* and $h^* = h_0/h_1$, are given in Table 2. This value also compares well to the $0.47 \le v^* \le 0.50$[2] reported for lock exchange problems and $v^* = 0.5$ in Eq. 7. The experimental $v^* = 0.44$ is lower than the $v^* = 0.5$ derived above, due to the mixing and the transient flow in this compartment. The average v* values for the slot, door and window decrease as the mixing increases. As the slot, door, or window size relative to h_1 decreases, $v^* \rightarrow 0$ from the Table 2 values. Similarly, increases in relative size cause $v^* \rightarrow 0.44$. As the aspect ratio (L/h_1) increases this limit may approach 0.50.

The error bars shown in Fig. 6 were calculated by compounding the errors for each parameter in Eqs. 1, 7 and 10. The large relative error bounds for the window opening are a result of the reduction in v*. The absolute error remains unchanged. The nondimensional height of the entering gravity current head, h* in Table 2, is based on visual observation from the video recordings of the experiments. The grid on the compartment seen in Figs. 4 and 5 is used to determine the heights. The grid lines are 25 mm apart and can be visually divided into four equal parts giving an accuracy of $\pm h_1/24$. The average head height of the gravity current is viewed over the distance 3L/4 to L to reduce any effects caused by the opening. The average head height did not change over the length of 3L/4 to L, within the accuracy of the measurement. The fully open head height, $h^* = 0.5$ is consistent with Eq. 5. The decreasing nondimensional head height with increasing mixing is also consistent with the $h^*<0.5$ suggested by Benjamin[1] for dissipative flows.

The Reynolds number shown in column 5 of Table 1 ranged from $939<Re<13407$. The Reynolds number is defined as:

$$Re = \frac{vh_0}{\nu}. \qquad (10)$$

For comparison with other gravity current results, h_0 is used in this definition. Over this range of Reynolds number the nondimensional velocities were found to be constant for each opening geometry. This Reynolds number independence is consistent with the results of Keulegan[12] and Barr[13] who found that the nondimensional velocity was strongly dependent on the Reynolds number for $Re < O(10^3)$ and independent for larger Re. Abraham and Vreugdenhil[14] indicate a slight increase in the nondimensional velocity for large Re. Simpson and Britter[15] indicate that the nondimensional velocity is either independent or only slightly

dependent on the Reynolds number for Re>O(10^3). For a 3m compartment fire, which is a candidate for a backdraft, the expected range would be $5 \times 10^3 < Re < 5 \times 10^4$. The independence suggested in the literature, and shown in Fig 6 and Table 1 for $10^3 < Re < 10^4$ indicates that the salt water results are directly applicable to typical fire compartments.

TABLE 1 - Summary of the salt water modeling results for the entering and exiting current. Results are shown for all four openings: full, slot, door, window.

	Entering Current				Exiting Current		
$\beta=\frac{(\rho_0-\rho_1)}{\rho_1}$	t_{in} (s)	v (m/s)	$v^*=\frac{v}{\sqrt{\beta g h_1}}$	$Re=\frac{vh_0}{\nu}$	t_{out} (s)	v (m/s)	$v^*=\frac{v_E}{\sqrt{\beta g h_1}}$
Full Opening							
0.010	5.80	0.053	0.43	3999	No Clearly defined exiting current was observed		
0.018	4.20	0.073	0.44	5523			
0.040	2.80	0.109	0.45	8284			
0.070	2.23	0.137	0.42	10401			
0.101	1.73	0.176	0.45	13407			
Slot Opening							
0.003	14.23	0.021	0.32	1239	32.53	0.02	0.33
0.005	10.43	0.029	0.34	1690	24.63	0.03	0.33
0.009	8.67	0.035	0.30	2033	20.47	0.03	0.30
0.010	8.57	0.036	0.29	2057	19.50	0.04	0.30
0.012	7.50	0.041	0.30	2350	17.87	0.04	0.30
0.022	5.70	0.053	0.30	3093	12.83	0.06	0.31
0.024	5.17	0.059	0.31	3410	12.13	0.06	0.31
0.030	4.43	0.069	0.32	3977	10.33	0.07	0.33
0.043	3.73	0.082	0.32	4726	9.27	0.08	0.30
0.043	3.67	0.083	0.33	4803	8.80	0.08	0.32
0.045	3.53	0.086	0.33	4990	8.60	0.08	0.32
0.050	3.33	0.092	0.33	5294	8.03	0.09	0.32
0.070	3.03	0.101	0.31	5818	6.93	0.10	0.32
0.075	3.00	0.102	0.30	5876	6.77	0.11	0.31
0.080	2.67	0.114	0.33	6602	6.40	0.11	0.32
0.090	2.50	0.122	0.33	7051	5.93	0.12	0.33
0.100	2.47	0.123	0.32	7137	5.73	0.12	0.32
Door Opening							
0.012	6.60	0.046	0.35	2319	16.37	0.04	0.32
0.026	4.50	0.068	0.34	3402	10.67	0.07	0.34
0.040	3.50	0.087	0.36	4374	8.73	0.08	0.33
0.055	2.97	0.103	0.36	5154	7.50	0.09	0.33
0.070	2.80	0.109	0.34	5467	6.57	0.11	0.33
0.085	2.43	0.125	0.35	6300	5.97	0.12	0.33
0.100	2.27	0.134	0.35	6744	5.50	0.13	0.33
Window Opening							
0.005	14.33	0.021	0.25	939	33.23	0.02	0.25
0.010	11.93	0.026	0.21	1128	27.63	0.03	0.21
0.025	7.00	0.044	0.23	1922	16.37	0.04	0.22
0.032	6.37	0.048	0.22	2112	14.80	0.05	0.22
0.040	5.47	0.056	0.23	2459	13.13	0.05	0.22
0.055	5.10	0.060	0.21	2638	11.53	0.06	0.22
0.070	4.23	0.072	0.22	3180	10.23	0.07	0.21
0.084	3.77	0.081	0.23	3568	9.23	0.08	0.22
0.102	3.33	0.092	0.23	4040	7.97	0.09	0.23

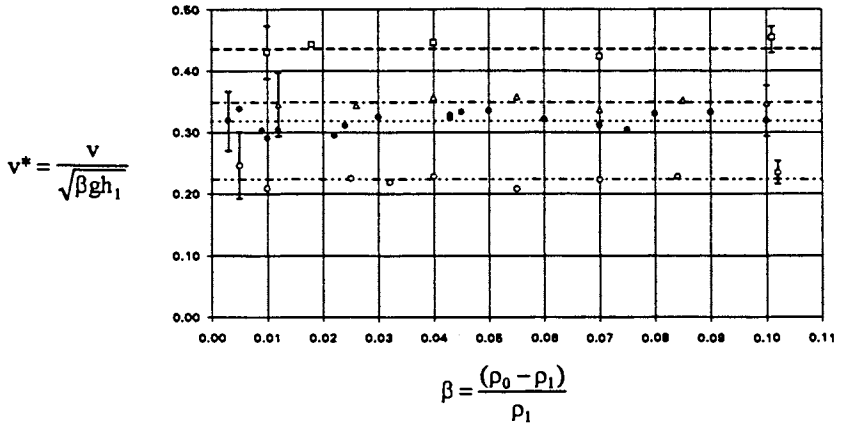

FIGURE 6 - Nondimensional velocity versus density difference ratio for four opening conditions. The □, •, o, Δ represent the data for the full, slot, window and door opening. The (– – –), (·····),(– ·–·–), (– · – ·), represent the average values for the full, slot, door and window geometries.

TABLE 2 - Average values for v * and h * calculated from the data reported in Table 1.

Opening	Full	Slot	Door	Window
$\bar{v}^*$	0.44	0.32	0.35	0.22
$\bar{h}^*$	0.50	0.38	0.33	0.29

CONCLUSIONS

This experimental work shows that the gravity current entering a fire compartment is both qualitatively and quantitatively similar to other naturally occurring gravity currents. The nondimensional velocity for the full opening compares well with the perfect fluid theory presented above. The structure of the entering gravity current head for the full open condition shows a shallow mixed region riding on the current at the interface. It also has the detailed features of steady state gravity currents, i.e. billows, lobes, and clefts. Entering currents for the slot, window, and door openings show a different gravity current structure with the mixed region occupying nearly the entire current due to the enhanced mixing near the opening. Similar detailed features appear as part of these currents.

The values of v* and h* obtained here for a variety of opening geometries, are independent of the density difference ratio, β. The exiting gravity current is also independent of β, and has a v* approximately equal to the entering current. These results can be applied to predict the time of ignition for a backdraft with compartment and opening geometries similar to the conditions reported here.

Additional research is necessary to investigate other compartment and opening geometries. Future work should focus on using larger aspect ratios (L/h_1) and a variety of opening ratios ($side/h_1$) as well as openings offset from the wall center line. Ceiling openings would elucidate the effects of firefighter ventilation tactics. More sophisticated instrumentation may also be used to measure concentrations within the current.

ACKNOWLEDGMENTS

National Institute of Standards and Technology, Building and Fire Research Laboratory, Grant No. 60NANB1D1168 and 60NANB3D1438 partially supported this work. Assistance from J. Fleischmann, W. MacCracken, A. Revenaugh, N. Dembsey, C. Grant and C. Caldwell is appreciated.

REFERENCES

[1] Benjamin, T.B., "Gravity Currents and Related Phenomenon", Journal of Fluid Mechanics, **31**, 209-248, 1968.
[2] Simpson, J.E., "Gravity Currents in the Laboratory, Atmosphere, and Ocean: Annual Review of Fluid Mechanics, **14**, 213-234, 1972.
[3] Steckler, K.D., Baum, H.R. and Quintere, J.G., "Salt Water Modeling of Fire Induced Flows in Multicompartment Enclosures", 21st Symposium (Int'l) on Combustion, 143-149, The Combustion Institute, Pittsburgh, PA, 1986.
[4] Chobotov, M. V., Zukoski, E. E. and Kubota, T., "Gravity Currents With Heat Transfer" NBS-GCR-87-522, National Bureau of Standards, Gaithersburg, MD, 1987.
[5] Fleischmann, C.M., Pagni, P.J. and Williamson, R.B., "Exploratory Backdraft Experiments", Fire Technology, **29**, 298-316, 1993.
[6] Britter, R.E. and Simpson, J.E., "Experiments on the Dynamics of a Gravity Current Head", Journal of Fluid Mechanics, **88**, 223-240, 1978.
[7] Kármán, T. von, "The Engineer Grapples with Nonlinear Problems", Bulletin of American Mathematics Society, **46**, 615, 1940.
[8] Breidenthal, R. "Structure in Turbulent Mixing Layers and Wakes Using a Chemical Reaction", Journal of Fluid Mechanics, **109**, 1-24, 1981.
[9] Simpson, J.E., "Effects of the Lower Boundary on the Head of a Gravity Current", Journal of Fluid Mechanics, **53**, 759-768, 1972.
[10] Simpson, J. E., "A Comparison Between Laboratory and Atmospheric Density Currents", Quarterly Journal of the Royal Meteorological Society, **95**, 758-765, 1969.
[11] Thorpe, S. A., "Experiments on Instability and Turbulence in a Stratified shear Flow", Journal of Fluid Mechanics, **61**, 731-751, 1973.
[12] Keukeganm G.H., "An Experimental Study of the Motion of Saline Water from Locks into Fresh Water Channels", National Bureau of Standards Report Number 5168, 1957.
[13] Barr, D.I.H., "Densimetric Exchange Flow in Rectangular Channels. III. Large Scale Experiments", Houille Blanche, **22**, 619-631, 1967.
[14] Abraham, G. and Vreugdenhill, C.B., "Discontinuities in Stratified Flow", Journal of Hydraulic Research, **9**, 292-308, 1971.
[15] Simpson, J.E. and Britter, R.E., "The Dynamics of the Gravity Current Advancing Over a Horizontal Surface", Journal of Fluid Mechanics, **94**, 477-495, 1979.